Short Article

Cell Stem Cell

Genomic Instability in Human Pluripotent Stem Cells Arises from Replicative Stress and Chromosome Condensation Defects

Graphical Abstract

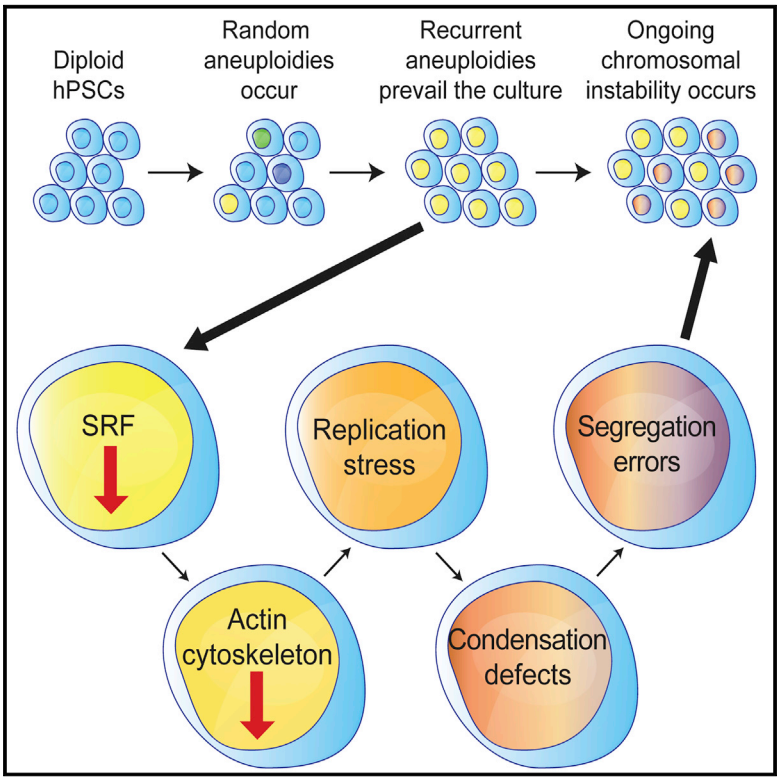

Authors

Noa Lamm, Uri Ben-David, Tamar Golan-Lev, Zuzana Storchová, Nissim Benvenisty, Batsheva Kerem

Correspondence

nissimb@mail.huji.ac.il (N.B.), batshevak@savion.huji.ac.il (B.K.)

In Brief

Lamm et al. identify a mechanism leading to the ongoing chromosomal instability observed in hPSCs harboring recurrent aneuplodies and which may induce instability in diploid hPSCs. They find that decreased SRF levels cause cytoskeletal impairments that perturb DNA replication and chromosomal condensation, resulting in chromosome segregation errors and genomic instability.

Highlights

- Aneuploid hPSCs exhibit replication stress resulting in condensation defects
- Partially condensed chromosomes lead to segregation errors in aneuploid hPSCs
- Levels of actin genes and their common regulator SRF in aneuploid hPSCs are decreased
- Cytoskeleton impairment perturbs replication and drives ongoing instability

Accession Numbers

GSE64647

Lamm et al., 2016, Cell Stem Cell *18*, 1–9
February 4, 2016
http://dx.doi.org/10.1016/j.stem.2015.11.003

CellPress

Please cite this article in press as: Lamm et al., Genomic Instability in Human Pluripotent Stem Cells Arises from Replicative Stress and Chromosome Condensation Defects, Cell Stem Cell (2016), http://dx.doi.org/10.1016/j.stem.2015.11.003

Cell Stem Cell
Short Article

CellPress

Genomic Instability in Human Pluripotent Stem Cells Arises from Replicative Stress and Chromosome Condensation Defects

Noa Lamm,[1] Uri Ben-David,[2,3] Tamar Golan-Lev,[2] Zuzana Storchová,[4] Nissim Benvenisty,[2,*] and Batsheva Kerem[1,*]
[1]Department of Genetics, The Hebrew University, Jerusalem, Israel
[2]Azrieli Center for Stem Cells and Genetic Research, Department of Genetics, The Hebrew University, Jerusalem, Israel
[3]Cancer Program, Broad Institute of Harvard and MIT, Cambridge, MA 02142, USA
[4]A Group Maintenance of Genome Stability, Max Planck Institute of Biochemistry, Am Klopferspitz 18, 82152 Martinsried, Germany
*Correspondence: nissimb@mail.huji.ac.il (N.B.), batshevak@savion.huji.ac.il (B.K.)
http://dx.doi.org/10.1016/j.stem.2015.11.003

SUMMARY

Human pluripotent stem cells (hPSCs) frequently acquire chromosomal aberrations such as aneuploidy in culture. These aberrations progressively increase over time and may compromise the properties and clinical utility of the cells. The underlying mechanisms that drive initial genomic instability and its continued progression are largely unknown. Here, we show that aneuploid hPSCs undergo DNA replication stress, resulting in defective chromosome condensation and segregation. Aneuploid hPSCs show altered levels of actin cytoskeletal genes controlled by the transcription factor SRF, and overexpression of SRF rescues impaired chromosome condensation and segregation defects in aneuploid hPSCs. Furthermore, SRF downregulation in diploid hPSCs induces replication stress and perturbed condensation similar to that seen in aneuploid cells. Together, these results suggest that decreased SRF expression induces replicative stress and chromosomal condensation defects that underlie the ongoing chromosomal instability seen in aneuploid hPSCs. A similar mechanism may also operate during initiation of instability in diploid cells.

INTRODUCTION

Human pluripotent stem cells (hPSCs) are commonly used in basic research and hold great promise for regenerative medicine based on their ability to differentiate to every cell type of the human body and their extensive self-renewal capacity. The indefinite self-renewal of hPSCs in vitro enables their prolonged propagation in culture but poses major challenges to their genome stability maintenance (reviewed in Weissbein et al., 2014). hPSCs proliferate fast and have a unique cell-cycle profile as well as aberrant cell-cycle checkpoints (Desmarais et al., 2012; Filion et al., 2009; Weissbein et al., 2014).

During culture propagation, hPSCs tend to acquire both structural and numerical aberrations (reviewed in Lund et al., 2012; Weissbein et al., 2014). Interestingly, numerical chromosomal aberrations in hPSCs tend to result in the acquisition of defined chromosomal aneuploidies. The typical changes are additional copies of chromosomes 12, and 17 X similar to changes found in germ cell tumors (Ben-David et al., 2011; Draper et al., 2004; Mayshar et al., 2010). The rapid proliferation of hPSCs, their inefficient cell-cycle checkpoints (Desmarais et al., 2012; Filion et al., 2009; Weissbein et al., 2014), and their tendency toward centrosomal amplification (Holubcová et al., 2011) suggest that aneuploidy may be actively promoted in these cells by impaired cell division mechanisms. While chromosomal aberrations are presumed to occur randomly, giving rise to karyotypically heterogeneous cultures (Peterson et al., 2008), only a few prevail and eventually take over the culture. Unlike somatic aneuploidies that often lead to altered metabolic properties and defects in cell growth (reviewed in Gordon et al., 2012), aneuploid hPSCs proliferate faster (Ben-David et al., 2014; Werbowetski-Ogilvie et al., 2009), and spend more time in S-phase (Ben-David et al., 2014) than their diploid counterparts. Karyotypic changes of chromosomes 12, and 17 confer hPSCs with a tumorigenic capacity (Baker et al., 2007). Moreover, the most common aberration in hPSCs, trisomy 12, induces profound changes in global gene expression of hPSCs, resulting in increased proliferation rate and tumorigenicity (Ben-David et al., 2014; Yang et al., 2008). Although the chromosomal aberrations that arise in hPSC cultures have been extensively described (Amps et al., 2011; Mayshar et al., 2010), the cellular mechanisms underlying their generation and the tumorigenic potential of hPSCs harboring recurrent aneuploidies remain largely unknown.

Aneuploidy is a hallmark of cancer (reviewed in Gordon et al., 2012). Aneuploidy in cancer can be induced by stress on DNA replication (Burrell et al., 2013). Replication stress is characterized by increased numbers of stalled and collapsed replication forks, leading to DNA damage. One mechanism underlying replication-induced chromosomal instability is the formation of anaphase bridges due to unreplicated or unresolved regions that restrain chromosome segregation by creating a physical link between sister chromatids (reviewed in Ozeri-Galai et al., 2012). In somatic cells, incomplete DNA replication activates checkpoints resulting in prolonged mitotic arrest to enable replication completion and damage repair. However, in hPSCs, incomplete DNA replication fails to generate the single-stranded

DNA regions necessary for checkpoint activation and repair initiation (Desmarais et al., 2012). Recurrent hPSC aneuploidies lead to increased proliferation and sensitivity to replication inhibitors (Ben-David et al., 2014). This suggests that hPSCs, and particularly aneuploid hPSCs, may be exceptionally vulnerable to replication stress. In addition to the hPSC-inherent deficiency in the intra-S checkpoints (Filion et al., 2009; Weissbein et al., 2014), the G2/M decatenation checkpoint is also deficient in these cells (Damelin et al., 2005). This checkpoint delays entry into mitosis until chromosomes have been detangled. Hence, in hPSCs, uncondensed chromosomes are able to form mitotic spindles and attempt anaphase separation of their entangled chromatids (Damelin et al., 2005). Proper chromosome condensation requires complete DNA replication (Gotoh, 2007). However, the effect of replication stress on chromosome condensation in hPSCs has yet to be studied.

Here we show that aneuploid hPSCs exhibit inherent perturbed DNA replication, resulting in a high prevalence of partially condensed metaphase chromosomes and chromosomal segregation errors. Moreover, our findings reveal that actin cytoskeleton impairment caused by reduced SRF levels underlies the ongoing chromosomal instability in hPSCs.

RESULTS

Perturbed DNA Replication Dynamics in Aneuploid hPSCs

We studied the replication dynamics in hPSCs with common aneuploidies. We focused on hPSCs with the gain of chromosomes 17q or 12, which are highly recurrent in cultured hPSCs and provide a selective propagation advantage (Baker et al., 2007). We investigated two pairs of diploid and trisomy-12-harboring hPSCs derived and cultured in the same laboratory using the same culture conditions: CSES10 and CSES22 (pair 1) (Ben-David et al., 2014; Biancotti et al., 2010) and HUES9 and HUES7 (pair 2) (Cowan et al., 2004). We validated that CSES10 and HUES9 exhibit normal karyotypes; CSES22 harbors trisomy 12 (hereafter referred to as T12-hPSCs); and HUES7 harbors trisomy of both chromosomes 12 and 17 (hereafter referred to as T12+17-hPSCs), which is commonly present in hPSCs (Baker et al., 2007; Draper et al., 2004; Mayshar et al., 2010). The replication dynamics was studied using the DNA combing approach (Figure 1A). First, we analyzed the DNA replication fork rate (Figures 1B–1D), which showed a significant increase in the percentage of very slow forks (0.75 kb/min and below) in T12-hPSCs and T12+17-hPSCs compared to their diploid counterparts (Figures 1B and 1C). The average replication rate of the two aneuploid hPSC lines was significantly lower than that of the two diploid counterparts (Figure 1D).

Slow fork progression leads to activation of additional origins to enable the completion of DNA replication (Ge et al., 2007). Hence, we studied origin density in diploid and in aneuploid hPSCs by measuring the distance between two sister forks (see Supplemental Experimental Procedures). This analysis showed a significant increase in the fraction of DNA fibers with a very short fork distance (100 kb and below) in aneuploid hPSCs compared to their diploid counterparts (Figures 1E and 1F). Furthermore, the average fork distance was significantly lower in aneuploid than in diploid hPSCs (Figure 1G). All together, our results show that the replication dynamics was perturbed in aneuploid hPSCs that had common chromosomal aberrations.

Impaired Metaphase Chromosome Condensation in Aneuploid hPSCs

Replication stress leads to gaps, constrictions, and local perturbations in chromosome condensation. Therefore, we studied the effect of the replication stress on chromosome condensation in aneuploid hPSCs. To our surprise, even after a long colcemid-induced metaphase arrest, metaphase spreads of hPSCs showed partially condensed entangled chromosomes in addition to the expected local condensation perturbations (Figures 2A and S1). Chromosome condensation in hPSCs ranged from fully condensed chromosomes to long and less compact chromosomes to fully entangled chromosomes. We classified the chromosomes into four groups according to their degree of condensation (1 represents normally condensed metaphases and 4 corresponds to fully entangled metaphases) (Figures 2A and S1). First, we studied the prevalence of condensation perturbations under normal conditions by analyzing the frequency of each subgroup in three aneuploid hPSCs (T12, T17, and T12+17), eight diploid hPSCs (both hESCs and iPSCs), and the following four diploid somatic cell lines: fibroblasts (BJ), epithelial cells (RPE and HCT116), and lymphocytes (GM07027). On average, ~95% of the metaphases from diploid somatic cells were scored in group 1, whereas only <5% were partially condensed (group 2). No entangled chromosomes were identified (groups 3 and 4) (Figures 2B and S2). In diploid hPSC metaphases, ~80% showed normal condensation (group 1), 10% were scored in group 2, and 10% were scored in groups 3 and 4. Strikingly, in metaphases of the aneuploid hPSCs, only 37% showed normal condensation, whereas condensation 2 was the largest subgroup (55%). Groups 3 and 4 accounted for ~20% of the metaphases in aneuploid hPSCs (Figure 2B).

Next we examined whether perturbed condensation also characterizes somatic trisomies. We analyzed two somatic cell lines (HCT116 and RPE) harboring trisomy 5 and 21, respectively. There was no significant difference between the aneuploid somatic cells and their diploid counterparts (Figures S2A and S2B). All together, these results show that perturbed condensation is extremely rare in both diploid and aneuploid somatic cells. However, these defects are more frequent in diploid hPSCs and are highly prevalent in aneuploid hPSCs, indicating that diploid hPSCs have an inherent tendency toward condensation defects, which is dramatically increased in aneuploid hPSCs. Proper chromosome condensation requires complete DNA replication (Gotoh, 2007). To investigate whether the high fraction of partially condensed metaphases in aneuploid hPSCs is a result of inherent replication stress, we used aphidicolin (APH), an inhibitor of DNA polymerase α and δ, to induce replication stress (Figures 2C and S2). APH treatment led to an increase in the number of partially condensed metaphases in all cell lines (Figures 2C and S2) and was positively correlated with the extent of APH-induced replication stress (Figures 2C and S2). However, while in diploid somatic fibroblasts (BJs) only ~17% of the metaphases were partially condensed even under severe replication stress conditions (0.4 μM APH), in diploid and aneuploid hPSCs under the same conditions, 60% and 80% of the metaphases were partially condensed, respectively (Figure 2C). These results

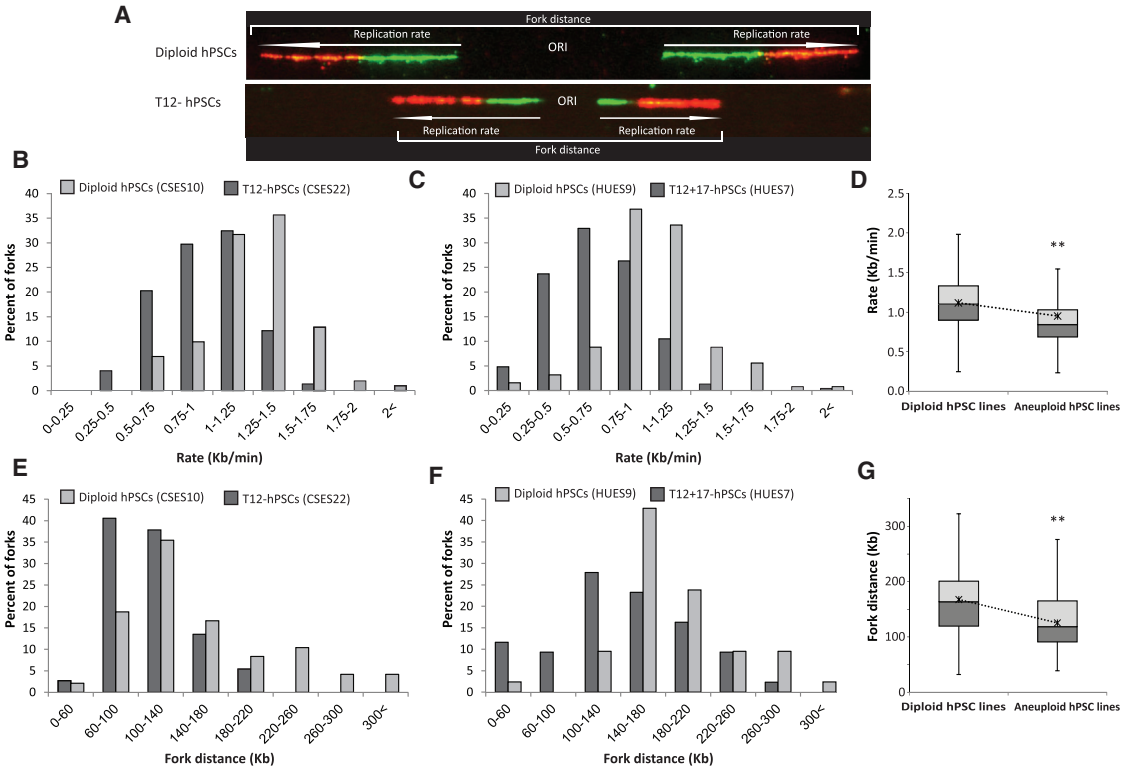

Figure 1. Perturbed Replication Dynamics in Aneuploid hPSCs

(A) Examples of single combed DNA molecules from diploid hPCSs and T12-hPSCs.

(B) Fork rate (kb/min) distribution. Light gray bars: diploid hPSCs (CSES10) (n = 111); dark gray bars: T12-hPSCs (CSES22) (n = 125) ($p < 5 \times 10^{-7}$).

(C) Fork rate (kb/min) distribution. Light gray bars: diploid hPSCs (HUES9) (n = 126); dark gray bars: T12+17-hPSCs (HUES7) (n = 132) ($p < 2.1 \times 10^{-8}$).

(D) Box plot with outliers of the average fork rate of four independent experiments. Diploid hPSC lines: average rate of four independent experiments, two in CSES10 and two in HUES9 (n = 498); aneuploid hPSC lines: average rate of four independent experiments, two in CSES22 and two in HUES7 (n = 512) ($p < 7 \times 10^{-6}$).

(E) Fork distance (kb) distribution. Light gray bars: diploid hPSCs (CSES10) (n = 67); dark gray bars: T12-hPSCs (CSES22) (n = 78) ($p < 1.6 \times 10^{-4}$).

(F) Fork distance (kb) distribution. Light gray bars: diploid hPSCs (HUES9) (n = 95); dark gray bars: T12+17-hPSCs (HUES7) (n = 81) ($p < 4.1 \times 10^{-4}$).

(G) Box plot with outliers of the average fork distance of four independent experiments. Diploid hPSC lines: average distance of four independent experiments, two in CSES10 and two in HUES9 (n = 278); aneuploid hPSC lines: average distance of four independent experiments, two in CSES22 and two in HUES7 (n = 251) ($p < 1.2 \times 10^{-4}$).

indicate that chromosome condensation in hPSCs is highly sensitive to replication stress. Notably, while under normal growth conditions condensation defects in all four analyzed diploid somatic cell lines were rare, under induced replication stress, a cell-type-specific sensitivity was found (Figures 2C and S2). In addition, the analysis of somatic diploid cells and their trisomic counterparts under stress conditions also did not show any significant difference in the prevalence of partially condensed metaphases (Figures S2A and S2B), indicating that the effect of aneuploidy on chromosome condensation is a characteristic feature of hPSCs.

Abnormal Anaphases and Genome Instability in Aneuploid hPSCs

Replication stress and partially condensed metaphases result in anaphase segregation errors characterized by anaphase bridges and lagging chromosomes (Downes et al., 1994; Burrell et al., 2013). Hence, we studied chromosome segregation in hPSCs. Anaphases with bridges and/or lagging chromosomes were defined as abnormal anaphases (Figure 2D). The analysis showed that under normal conditions, abnormal anaphases were significantly more frequent in hPSCs than in somatic cells (Figure 2E). Moreover, there were significantly more abnormal anaphases in aneuploid than in diploid hPSCs (Figure 2E), further supporting the findings that aneuploid hPSCs experience replication stress that leads to perturbation of chromosome condensation during metaphase.

If the identified characteristics of aneuploid cells are causal to aneuploidy, one would expect that aneuploid cells would become more aneuploid as these factors continue to act. In fact, hPSCs with T12 or T17 often harbor additional aberrations and become more aneuploid with time (Amps et al., 2011; Baker et al., 2007). To further examine instability in aneuploid hPSCs, six of our diploid hPSC cell lines were karyotyped. Only 4/140 karyotyped metaphases (2.9%) showed chromosomal aberrations (Table S1). In contrast, three aneuploid hPSC lines harboring trisomy 12 or 17 were highly unstable: in 25/74 (34%) analyzed metaphases, additional aberrations were present ($p < 0.0001$) (Table S2). These data strongly support the notion that aneuploid cells are highly unstable compared to their

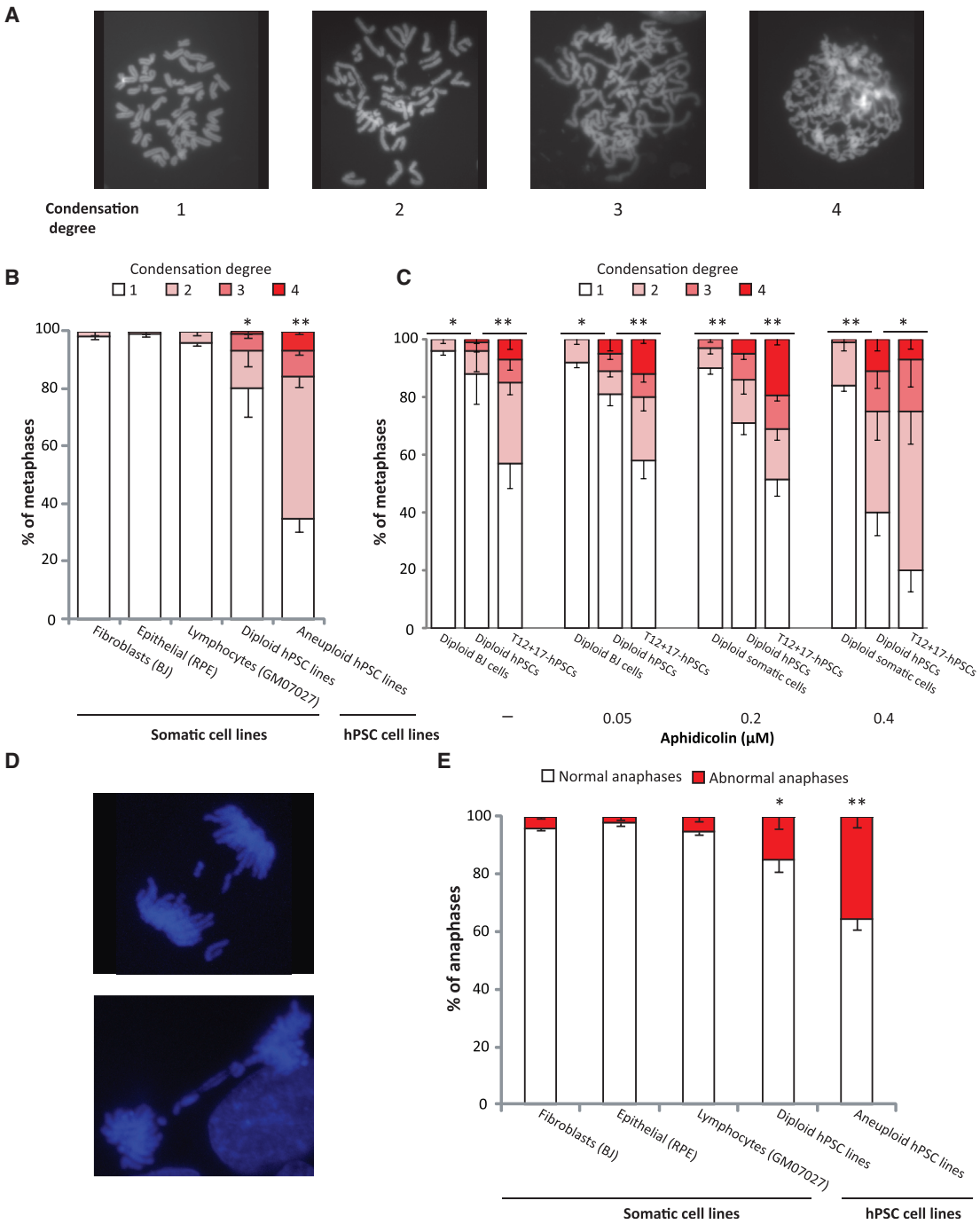

Figure 2. Replication Stress in Aneuploid hPSCs Results in Impaired Chromosome Condensation and a High Rate of Segregation Errors

(A) Representative examples of the four condensation groups.

(B) Percentage of metaphases in each group. (Data are represented as mean ± SEM.) Diploid somatic cell lines: fibroblasts (BJ, immortalized foreskin fibroblast cells, n = 115), epithelial cells (RPE, retinal pigment epithelial cells, n = 84), and lymphocytes (GM07027, lymphobalstoid cell line, n = 78). Diploid hPSC lines, five diploid hESC lines (HUES9, CSES10, H9, CSES19, and CSES26), and two diploid hiPSC lines (BJ-hiPSC28 and BJ-hiPSC94) (n = 598) are shown. The average result of all seven cell lines is shown. Aneuploid hPSC lines were HUES7, CSES22, and CSES8 (n = 280). The average result of the three aneuploid hPSC lines is shown.

(C) Percentage of metaphases in each condensation group under the indicated APH concentration. (Data are represented as mean ± SEM.) Diploid somatic cells: BJ (n > 120 for each concentration); diploid hPSCs: HUES9 (n > 120 for each concentration); aneuploid hPSCs: HUES7 (n > 120 for each concentration).

(D) Representative examples of abnormal anaphases from HUES7 under normal culture conditions.

(E) Percentage of abnormal anaphases grown under normal conditions. (Data are represented as mean ± SEM.) Diploid somatic cell lines were BJ (n = 69), RPE (n = 73), and GM07027 (n = 81). Diploid hPSC lines were HUES9 and CSES10 (n = 240). Aneuploid hPSC lines were HUES7 and CSES22 (n = 236). The results are the average of the two lines. *$p < 0.005$, **$p < 0.001$.

diploid counterparts and experience ongoing chromosomal instability.

Reduced Expression of Actin Cytoskeleton Genes in Aneuploid hPSCs

We next investigated the molecular basis of the marked perturbations in DNA replication, chromosome condensation, and segregation by comparing the global gene expression patterns of diploid and aneuploid hPSCs. We compiled a database of 31 expression microarrays of diploid hPSCs from nine studies, 8 microarrays of aneuploid hPSCs with culture-acquired trisomy 12 from five studies, and 4 microarrays of aneuploid hPSCs with culture-acquired trisomy 17 from four studies (Table S3). One of the samples was from cells with trisomy 12 and 17, and another was from cells with trisomies 12 and 3 (Table S3). Previous gene expression analyses have focused on the effect of specific chromosomal aberrations on global gene expression patterns (Ben-David et al., 2014). In contrast, here we focused on the gene expression changes that occur in culture-adapted aneuploid hPSCs regardless of the specific aberration, since the replication, condensation, and segregation changes observed in aneuploid hPSCs did not depend on the type of aberration (Figures 1 and 2).

We performed a gene set enrichment analysis (GSEA) with all expressed genes to identify pathways that are perturbed in aneuploid hPSCs. This analysis revealed that genes in the DNA replication and chromosome condensation pathways were among the most downregulated groups of genes in the aneuploid hPSCs (Figures 3A and 3B). We next subjected the lists of the 100 most upregulated and the 100 most downregulated probe sets in aneuploid hPSCs (compared to diploid hPSCs) to DAVID functional annotation enrichment analysis. Importantly, probe sets were required to be differentially expressed in both hPSCs with trisomy 12 and 17 so that genes with altered expression in only one type of aberration were excluded from the analysis (see Experimental Procedures). Whereas the list of genes upregulated in aneuploid hPSCs was not significantly enriched with any cellular process, the list of genes downregulated in recurrent aneuploid hPSCs was significantly enriched with actin cytoskeleton-related annotations (Figure 3C). The differentially expressed genes in this group included several of the hallmark cytoskeleton genes (Figure 3D). The actin cytoskeleton is highly important for chromosome condensation and segregation during mitosis (Gachet et al., 2001); therefore, its perturbation in aneuploid hPSCs may underlie the phenotype observed in these cells.

We next performed a PRIMA analysis to identify transcription factors whose binding sites were enriched in the list of the 100 most downregulated probe sets. The only significant enrichment was found for the targets of the serum response factor (*SRF*) transcription factor (Figure 3E). *SRF* controls transcription of many cellular ''immediate-early'' genes whose expression is activated by mitogenic stimuli such as serum and growth factor addition (Esnault et al., 2014; Spencer et al., 1999). In line with its role as a positive regulator, and the downregulation of its targets in aneuploid hPSCs, we found *SRF* itself to be downregulated in hPSCs with either trisomy 12 or trisomy 17 (Figure S3A).

Next, we validated *SRF* downregulation in T12 and T12+17-hPSCs by RT-qPCR. Both cell lines displayed a significant reduction in their *SRF* expression level compared to diploid cell lines (Figure 3F). Western blot analysis showed also a reduction in the SRF protein level (Figure 3G). Next, using RT-qPCR, we confirmed the expression levels of several actin cytoskeletal genes that are *SRF* targets and were significantly downregulated in the microarray data. Consistent with the reduced *SRF* levels found in T12 and T12+17-hPSCs, we found a significant reduction in *SRF*-targeted actin cytoskeletal genes in both cell lines (Figures 3H and S3B).

SRF regulates genes via combinatorial interaction with additional transcription factors, cofactors, and signaling pathways. We next studied the expression level of additional known targets of *SRF* involved in different *SRF*-controlled pathways (Esnault et al., 2014) in diploid and aneuploid hPSCs. Only two pathways were significantly ($p < 0.01$) downregulated in aneuploid hPSCs: the ''associated with F-actin and actomyosin'' and the ''focal adhesion'' pathways, both related to the actin cytoskeleton (Table S4). These results indicate that not all *SRF* targets are equally sensitive to a reduction in its expression.

SRF Overexpression Rescues Impaired Metaphase Chromosome Condensation and Abnormal Anaphases in Aneuploid hPSCs

Next, we studied whether *SRF* overexpression in aneuploid hPSCs was sufficient to rescue the impaired chromosome condensation and segregation perturbations. We stably transfected T12-hPSCs with an *SRF* plasmid. SRF protein levels were measured, and two clones showing significant increased SRF levels were selected for further analysis (Figure 3I). *SRF* overexpression in these aneuploid hPSCs led to a significant decrease in the prevalence of impaired chromosome condensation (Figure 3G). Importantly, in the *SRF*-overexpressing aneuploid hPSCs, the prevalence of perturbed condensation was significantly reduced ($p < 0.01$) and reached levels similar to those found in diploid hPSCs. Similarly, the prevalence of abnormal anaphases was significantly reduced following *SRF* overexpression (Figures S3C and S3D). These results show that *SRF* overexpression is sufficient to significantly rescue the abnormal phenotype of aneuploid hPSCs.

Downregulation of *SRF* Leads to Replication Stress and Impaired Metaphase Chromosome Condensation in Diploid hPSCs

We then studied whether reduced *SRF* expression is sufficient to induce replication stress and perturbation in chromosome condensation. We transfected diploid hPSCs with siRNA smart pool against *SRF*. Western blot analysis showed an ~50% reduction in the SRF levels (Figure S4A). *SRF* downregulation led to a significant reduction in the average fork rate and distance (Figures 4A and 4B and S4B and S4C). Subsequently we treated diploid hPSCs with APH for 24 hr and found that APH did not affect SRF protein levels (Figure S4D), indicating that replication stress was not the initiating event leading to insufficient SRF.

Last, we studied the effect of *SRF* downregulation on chromosome condensation. Analysis of metaphase spreads revealed a significant increase in the percentage of partially condensed metaphases in *SRF*-siRNA-transfected diploid hPSCs (Figure 4C), clearly showing that reduced SRF levels in diploid hPSCs result in the replication stress and impaired chromosome condensation that characterize aneuploid hPSCs.

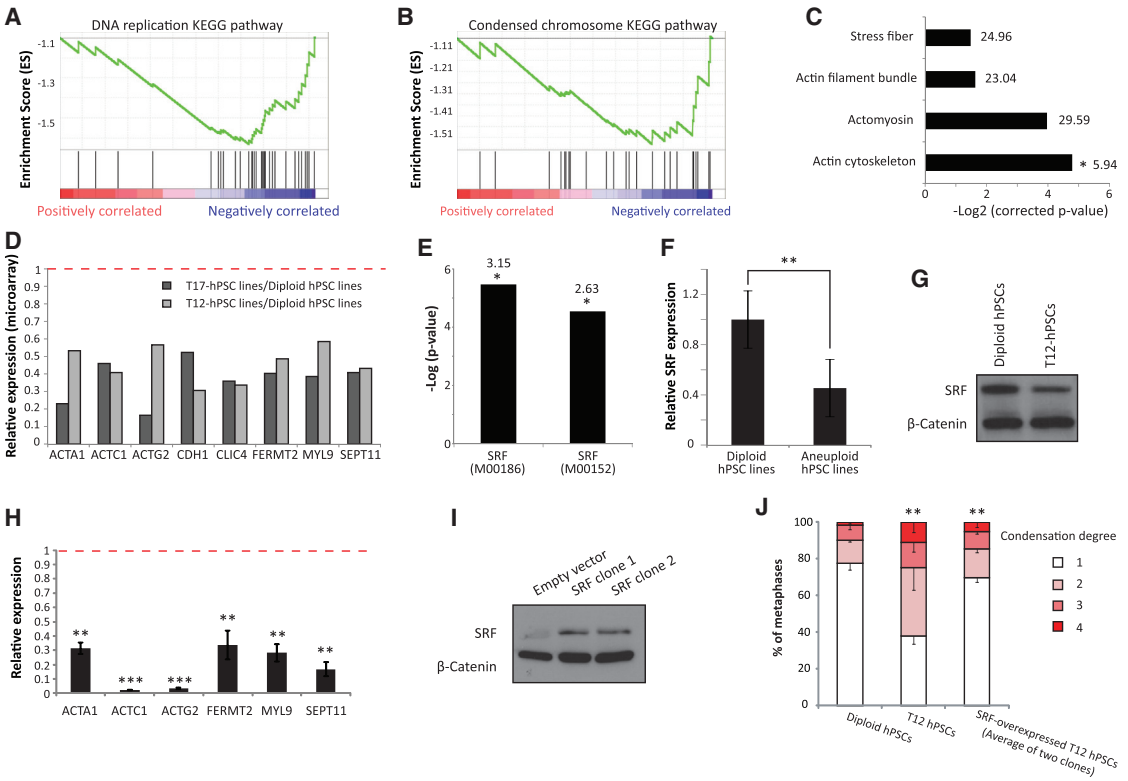

Figure 3. Gene Expression Analysis Reveals Impaired Actin Cytoskeleton Predicted to Result from *SRF* Downregulation

(A) GSEA enrichment plot for the DNA replication KEGG pathway, created by comparing diploid and aneuploid hPSCs for all expressed genes (normalized enrichment score [NES] = −1.35).

(B) GSEA enrichment plot for the condensed chromosome KEGG pathway, created by comparing diploid and aneuploid hPSCs for all expressed genes (NES = −1.43).

(C) Perturbed biological pathways identified in aneuploid hPSCs, based on DAVID functional annotation enrichment analysis of the 100 most downregulated expressed genes between aneuploid and diploid hPSCs. Enrichment fold-ratios are presented next to the bars, *p = 0.036 after Benjamini correction for multiple testing.

(D) Relative gene expression levels, as measured by expression microarrays, of the eight genes that belong to the "actin cytoskeleton" annotation identified in (C).

(E) PRIMA promoter enrichment analysis of the 100 most downregulated expressed genes in aneuploid hPSCs.

(F) The levels of *SRF* transcripts were measured by RT-qPCR. (Data are represented as mean ± SEM.) Diploid hPSC lines: average of the relative *SRF* expression from four independent experiments (two performed in HUES9 and two in CSES10); aneuploid hPSC lines: average of the relative *SRF* expression from four independent experiments (two performed in HUES7 and two in CSES22). Values were normalized against transcripts of the TBP gene. *$p < 0.05$, **$p < 0.01$, ***$p < 0.001$.

(G) Immunoblotting with anti-SRF and anti-β catenin antibodies, with their protein levels measured in the diploid hPSC line CSES10 and the aneuploid hPSC line CSES22.

(H) The relative level of transcripts of six genes that belong to the "actin cytoskeleton" annotation were measured by RT-qPCR. Data are represented as mean ± SEM of the relative expression in CSES22 compared to CSES10 from three independent experiments. Values were normalized against transcripts of the TBP gene. *$p < 0.05$, **$p < 0.01$, ***$p < 0.001$.

(I) Protein extracts from CSES22 expressing an empty vector (Empty vector) and extracts from two CSES22 clones transfected with an *SRF* plasmid (Clone 1 and Clone 2) prepared 1 week post selection and analyzed by western blot with anti-SRF and anti-β catenin antibodies.

(J) Percentage of metaphases in each condensation group. Data are represented as mean ± SEM of two independent experiments (one from each clone) with CSES10 (n = 121), CSES22 (n = 154), and aneuploid hPSCs overexpressing SRF (n = 225). **$p < 0.01$.

Impaired Organization and Transcription of Actins Lead to Replication Stress and Defects in Chromosome Condensation and Drive Genome Instability in Diploid hPSCs

In order to study the effect of actin cytoskeletal genes on DNA replication and chromosome condensation, we cultured diploid hPSCs in a medium containing Latrinculin B (Lat B), an inhibitor of actin polymerization. Lat B increases the level of monomeric actin, which inhibits the formation of the SRF-MRTF complex required for the transcription of actin and actin-related genes. Therefore, Lat B indirectly inhibits transcription of the SRF-MRTF targets only. Lat B led to a significant reduction in the average fork rate and fork distance (Figures 4D and 4E and S4E and S4F), suggesting that disruption of actin polymerization leads to replication stress in diploid hPSCs.

Next, we studied the effect of Lat B on chromosome condensation during metaphase. Cells cultured in Lat B showed a significant increase in the percentage of partially condensed metaphases (Figure 4F). Moreover, the percentage of metaphases in condensation groups 3 and 4, which were very rare

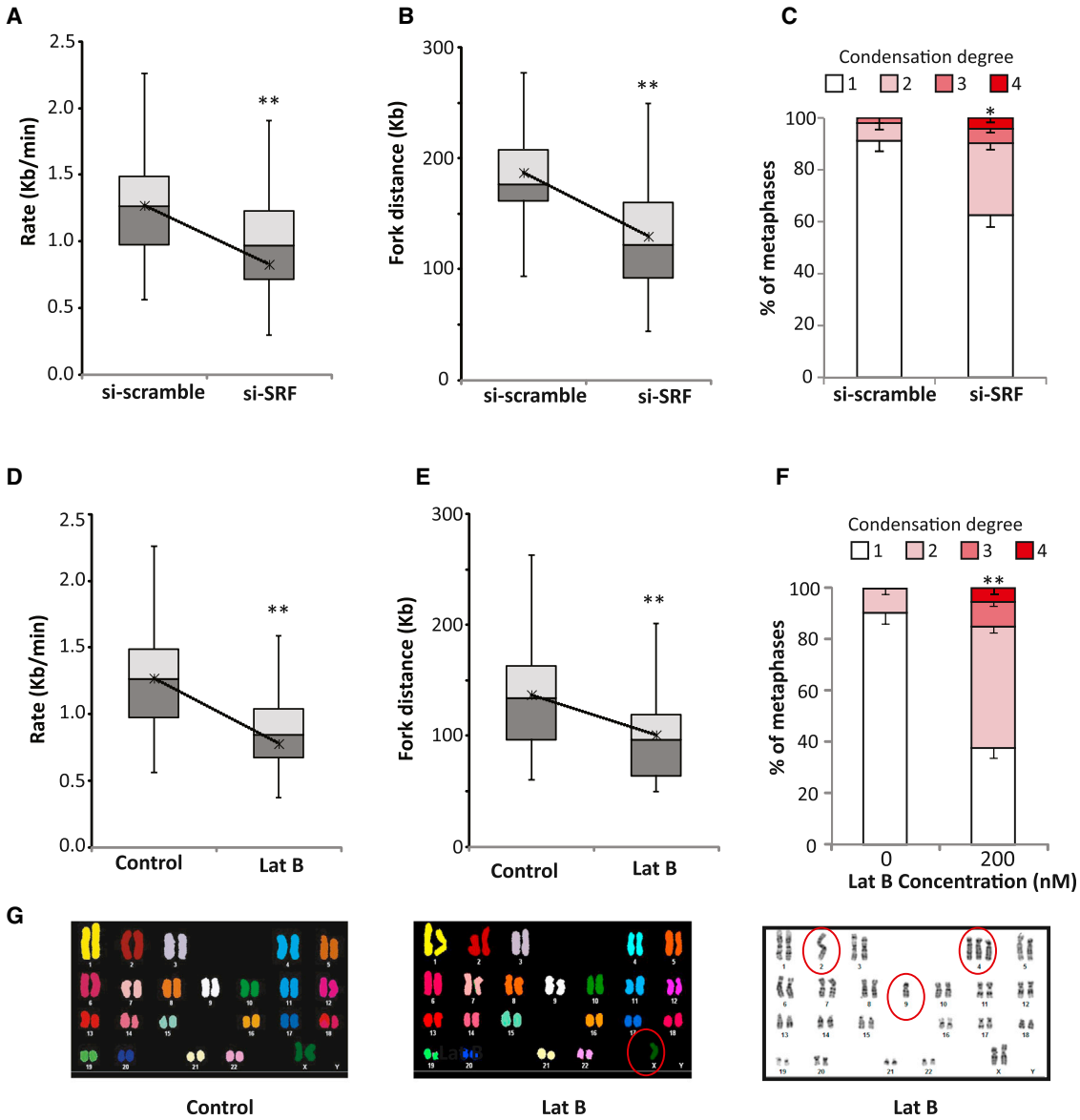

Figure 4. Perturbed Actin Cytoskeleton Organization and Transcription Leads to Replication Stress and Impaired Metaphase Chromosome Condensation and Drives Genome Instability in Diploid hPSCs

(A) Box plot representation of the average fork rate (kb/min) from three independent experiments. CSES10 was transfected with si-scramble (n = 308) or si-SRF (n = 309) ($p < 5.3 \times 10^{-8}$).

(B) Box plot of the average fork distance (kb) from three independent experiments. CSES10 was transfected with si-scramble (n = 200) or si-SRF (n = 212) ($p < 2.5 \times 10^{3}$).

(C) Percentage of metaphases in each condensation group. Data are represented as mean ± SEM of three independent experiments. CSES10 was transfected with si-scramble (n = 256) or si-SRF (n = 283) *$p < 0.05$.

(legend continued on next page)

in untreated hPSCs, increased significantly in Lat-B-treated cells (Figure 4F). These results show that inhibition of actin polymerization by Lat B leads to a dramatic increase in partially condensed metaphases in diploid hPSCs, similar to the level found in untreated aneuploid hPSCs (Figure 2).

An important question emerging from these results is whether perturbation in actin function is sufficient to induce ongoing chromosomal instability. For this we karyotyped the CSES10 diploid hPSC line after Lat B treatment. As described above, chromosomal aberrations in diploid hPSCs are highly uncommon, and in CSES10 cells specifically, all untreated metaphases were diploid (Table S1). In contrast, after Lat B treatment, 20% of the CSES10 metaphases were aneuploid (Figure 4G) ($p < 0.01$). These data show that perturbation in actin cytoskeleton function by Lat B drives genome instability in diploid hPSCs.

DISCUSSION

Here we identified a mechanism leading to the ongoing chromosomal instability in hPSCs that harbor recurrent aneuploidies. This may explain the propensity of these cells to acquire a complex karyotype. We showed that the DNA replication dynamics in aneuploid hPSCs is perturbed, resulting in a high prevalence of partially condensed metaphase chromosomes, chromosomal segregation errors, and genome instability.

Why does replication stress in hPSCs result in a robust phenotype of partially condensed metaphases, whereas in somatic cells it only results in local perturbations in chromosome condensation? A reasonable explanation is the different efficiencies of checkpoint activations between somatic cells and hPSCs. In somatic cells, the effective intra-S and G2/M checkpoints arrest cells whose replication was perturbed and incomplete. The only cells that manage to escape these checkpoints suffer mild replication perturbation resulting in local condensation defects at these sites. hPSCs, however, are not arrested by the intra-S and G2/M checkpoints and proceed along the cell cycle even if their replication is significantly perturbed, resulting in a robust phenotype of partially condensed metaphases.

Our bioinformatics analyses revealed reduced transcription levels of actin cytoskeleton genes and their common transcription factor *SRF* in aneuploid hPSCs. Moreover, diploid hPSCs treated with Lat B, an inhibitor of both actin polymerization and *SRF*-dependent transcription, recapitulated the replication and condensation defects in untreated aneuploid hPSCs. These results indicate that the perturbation of actin transcription and organization is the mechanism leading to instability and ongoing chromosomal aberrations in aneuploid hPSCs.

Based on the results presented here, we suggest a model for the cellular events leading to ongoing chromosomal instability in aneuploid hPSCs (Figure 4H). According to this model, *SRF* downregulation leads to downregulation of actin-cytoskeleton genes, leading to replication stress and partially condensed metaphases. This further leads to abnormal anaphases and provides the cells with the ability to acquire additional aberrations (Figure 4H).

SRF was first identified in studies that investigated the response of fibroblasts to serum addition. Hence, our results raise the question of whether certain culture conditions (e.g., growth factor starvation) might induce genetic instability in hPSC cultures by reducing the expression of *SRF*. Importantly, culturing hPSCs with bFGF-depleted medium resulted in decreased levels of SRF (Figure S4G). In our study the diploid and aneuploid hPSCs were grown in the exact same medium; hence this cannot account for the different SRF levels found between them. Nevertheless, these results emphasize the importance of optimal culture conditions to protect SRF levels and genome stability.

Here we show that in hPSCs, replication stress results in chromosome condensation defects. Therefore, the consequences of replication stress in hPSCs might be even more deleterious than in somatic cells and may also operate during initiation of instability in diploid hPSCs. In summary, our results suggest a mechanism that might also be relevant for the development of germ cell tumors (and potentially other tumor types with impaired intra-S or decatenation checkpoints).

EXPERIMENTAL PROCEDURES

Global Gene Expression Analysis

Total RNA was extracted from undifferentiated hPSCs using the RNeasy mini kit (QIAGEN). RNA was subjected to Human Genome U133 Plus 2.0 microarray platform (Affymetrix); original microarray data are accessible at the NCBI Gene Expression Omnibus (GEO) database under the accession number GEO: GSE64647 (http://www.ncbi.nlm.nih.gov/geo/). In addition, microarray data of undifferentiated hPSCs were downloaded from the GEO database (detailed in Table S3). Arrays were normalized using MAS5 algorithm in the Affymetrix Expression Console. Probe sets absent in both diploid and aberrant hPSCs were filtered out by the MAS5 Absent/Present call. Probe sets with expression values below 100 were raised to this level. The karyotype of the analyzed cell lines was validated by virtual karyotyping. Lists of differentially expressed genes between diploid hPSCs and aneuploid hPSCs were derived by applying the following thresholds: minimal fold-change between diploid and aneuploid hPSCs, fold-change between diploid and T12-hPSCs < 0.8, fold-change between diploid and T17-hPSCs < 0.8. To detect significantly over-represented KEGG pathways, we subjected the lists of differentially expressed genes to the DAVID functional annotation clustering tool (https://david.ncifcrf.gov/). To detect significantly over-represented transcription binding sites, we subjected the lists of differentially expressed genes to PRIMA analysis (http://acgt.cs.tau.ac.il/prima/). GSEA was performed using the GSEA software (http://www.broadinstitute.org/gsea/index.jsp).

ACCESSION NUMBERS

Original microarray data are accessible at the NCBI GEO database under the accession number GEO: GSE64647 (http://www.ncbi.nlm.nih.gov/geo/).

(D) Box plot representation of the average fork rate from three independent experiments in CSES10, with (n = 325) and without (n = 319) exposure to 200 nM Lat B for 24 hr ($p < 7 \times 10^{-10}$).

(E) Box plot representation of the average fork distance (kb) from three independent experiments in CSES10, with (n = 325) and without (n = 319) exposure to 200 nM Lat B for 24 hr ($p < 3.6 \times 10^{-6}$).

(F) Percentage of metaphases in each condensation group. Data are represented as mean ± SEM of three independent experiments in CSES10, with (n = 275) and without (n = 296) exposure to 200 nM Lat B for 24 hr. **$p < 0.01$.

(G) Examples of SKY and Giemsa karyotypes of CSES10 metaphases with (n = 60) and without (n = 30) exposure to 150 nM Lat B for 24 hr. **$p < 0.01$.

(H) A model of the cellular events leading to ongoing chromosomal instability in aneuploid hPSCs.

SUPPLEMENTAL INFORMATION

Supplemental Information for this article includes four figures, four tables, and Supplemental Experimental Procedures and can be found with this article online at http://dx.doi.org/10.1016/j.stem.2015.11.003.

AUTHOR CONTRIBUTIONS

N.L., U.B.-D., N.B., and B.K. conceived and designed the experiments. N.L. conducted the experiments. U.B.-D. performed computational analysis. T.G.-L. assisted with karyotyping and tissue culture. Z.S. provided aneuploid somatic cells. N.L., U.B.-D., N.B., and B.K. analyzed the data and wrote the paper.

ACKNOWLEDGMENTS

This research was partially supported by the Israel Science Foundation (grant No. 176/11), the Israeli Cancer Association, the Chief Scientist's Office of the Israel Ministry of Health and the Israeli Centers of Research Excellence (I-CORE), and Gene Regulation in Complex Human Disease, Center No 41/11 to B.K. The Azrieli Foundation, the Rosetrees Trust, and the Israel Science Foundation (grant number 269/12) supported N.B. N.B. is the Herbert Cohn Chair in Cancer Research. N.L. was supported by a postdoctoral fellowship from the Israel Cancer Research Fund. U.B.-D. was supported by a Human Frontiers Science Program (HFSP) postdoctoral fellowship. We thank Aline Sewo Pires de Campos from the Storchová laboratory who is mostly responsible for the construction, determination, and maintenance of the somatic trisomies cell lines.

Received: January 12, 2015
Revised: August 31, 2015
Accepted: November 5, 2015
Published: December 3, 2015

REFERENCES

Amps, K., Andrews, P.W., Anyfantis, G., Armstrong, L., Avery, S., Baharvand, H., Baker, J., Baker, D., Munoz, M.B., Beil, S., et al.; International Stem Cell Initiative (2011). Screening ethnically diverse human embryonic stem cells identifies a chromosome 20 minimal amplicon conferring growth advantage. Nat. Biotechnol. *29*, 1132–1144.

Baker, D.E.C., Harrison, N.J., Maltby, E., Smith, K., Moore, H.D., Shaw, P.J., Heath, P.R., Holden, H., and Andrews, P.W. (2007). Adaptation to culture of human embryonic stem cells and oncogenesis in vivo. Nat. Biotechnol. *25*, 207–215.

Ben-David, U., Mayshar, Y., and Benvenisty, N. (2011). Large-scale analysis reveals acquisition of lineage-specific chromosomal aberrations in human adult stem cells. Cell Stem Cell *9*, 97–102.

Ben-David, U., Arad, G., Weissbein, U., Mandefro, B., Maimon, A., Golan-Lev, T., Narwani, K., Clark, A.T., Andrews, P.W., Benvenisty, N., and Carlos Biancotti, J. (2014). Aneuploidy induces profound changes in gene expression, proliferation and tumorigenicity of human pluripotent stem cells. Nat. Commun. *5*, 4825.

Biancotti, J.-C., Narwani, K., Buehler, N., Mandefro, B., Golan-Lev, T., Yanuka, O., Clark, A., Hill, D., Benvenisty, N., and Lavon, N. (2010). Human embryonic stem cells as models for aneuploid chromosomal syndromes. Stem Cells *28*, 1530–1540.

Burrell, R.A., McClelland, S.E., Endesfelder, D., Groth, P., Weller, M.-C., Shaikh, N., Domingo, E., Kanu, N., Dewhurst, S.M., Gronroos, E., et al. (2013). Replication stress links structural and numerical cancer chromosomal instability. Nature *494*, 492–496.

Cowan, C.A., Klimanskaya, I., McMahon, J., Atienza, J., Witmyer, J., Zucker, J.P., Wang, S., Morton, C.C., McMahon, A.P., Powers, D., and Melton, D.A. (2004). Derivation of embryonic stem-cell lines from human blastocysts. N. Engl. J. Med. *350*, 1353–1356.

Damelin, M., Sun, Y.E., Sodja, V.B., and Bestor, T.H. (2005). Decatenation checkpoint deficiency in stem and progenitor cells. Cancer Cell *8*, 479–484.

Desmarais, J.A., Hoffmann, M.J., Bingham, G., Gagou, M.E., Meuth, M., and Andrews, P.W. (2012). Human embryonic stem cells fail to activate CHK1 and commit to apoptosis in response to DNA replication stress. Stem Cells *30*, 1385–1393.

Downes, C.S., Clarke, D.J., Mullinger, A.M., Giménez-Abián, J.F., Creighton, A.M., and Johnson, R.T. (1994). A topoisomerase II-dependent G2 cycle checkpoint in mammalian cells/. Nature *372*, 467–470.

Draper, J.S., Smith, K., Gokhale, P., Moore, H.D., Maltby, E., Johnson, J., Meisner, L., Zwaka, T.P., Thomson, J.A., and Andrews, P.W. (2004). Recurrent gain of chromosomes 17q and 12 in cultured human embryonic stem cells. Nat. Biotechnol. *22*, 53–54.

Esnault, C., Stewart, A., Gualdrini, F., East, P., Horswell, S., Matthews, N., and Treisman, R. (2014). Rho-actin signaling to the MRTF coactivators dominates the immediate transcriptional response to serum in fibroblasts. Genes Dev. *28*, 943–958.

Filion, T.M., Qiao, M., Ghule, P.N., Mandeville, M., van Wijnen, A.J., Stein, J.L., Lian, J.B., Altieri, D.C., and Stein, G.S. (2009). Survival responses of human embryonic stem cells to DNA damage. J. Cell. Physiol. *220*, 586–592.

Gachet, Y., Tournier, S., Millar, J.B., and Hyams, J.S. (2001). A MAP kinase-dependent actin checkpoint ensures proper spindle orientation in fission yeast. Nature *412*, 352–355.

Ge, X.Q., Jackson, D.A., and Blow, J.J. (2007). Dormant origins licensed by excess Mcm2-7 are required for human cells to survive replicative stress. Genes Dev. *21*, 3331–3341.

Gordon, D.J., Resio, B., and Pellman, D. (2012). Causes and consequences of aneuploidy in cancer. Nat. Rev. Genet. *13*, 189–203.

Gotoh, E. (2007). Visualizing the dynamics of chromosome structure formation coupled with DNA replication. Chromosoma *116*, 453–462.

Holubcová, Z., Matula, P., Sedláčková, M., Vinarský, V., Doležalová, D., Bárta, T., Dvořák, P., and Hampl, A. (2011). Human embryonic stem cells suffer from centrosomal amplification. Stem Cells *29*, 46–56.

Lund, R.J., Närvä, E., and Lahesmaa, R. (2012). Genetic and epigenetic stability of human pluripotent stem cells. Nat. Rev. Genet. *13*, 732–744.

Mayshar, Y., Ben-David, U., Lavon, N., Biancotti, J.-C., Yakir, B., Clark, A.T., Plath, K., Lowry, W.E., and Benvenisty, N. (2010). Identification and classification of chromosomal aberrations in human induced pluripotent stem cells. Cell Stem Cell *7*, 521–531.

Ozeri-Galai, E., Bester, A.C., and Kerem, B. (2012). The complex basis underlying common fragile site instability in cancer. Trends Genet. *28*, 295–302.

Peterson, S.E., Westra, J.W., Paczkowski, C.M., and Chun, J. (2008). Chromosomal mosaicism in neural stem cells. Methods Mol. Biol. *438*, 197–204.

Spencer, J.A., Major, M.L., and Misra, R.P. (1999). Basic fibroblast growth factor activates serum response factor gene expression by multiple distinct signaling mechanisms. Mol. Cell. Biol. *19*, 3977–3988.

Weissbein, U., Benvenisty, N., and Ben-David, U. (2014). Quality control: Genome maintenance in pluripotent stem cells. J. Cell Biol. *204*, 153–163.

Werbowetski-Ogilvie, T.E., Bossé, M., Stewart, M., Schnerch, A., Ramos-Mejia, V., Rouleau, A., Wynder, T., Smith, M.-J., Dingwall, S., Carter, T., et al. (2009). Characterization of human embryonic stem cells with features of neoplastic progression. Nat. Biotechnol. *27*, 91–97.

Yang, S., Lin, G., Tan, Y.-Q., Zhou, D., Deng, L.-Y., Cheng, D.-H., Luo, S.-W., Liu, T.-C., Zhou, X.-Y., Sun, Z., et al. (2008). Tumor progression of culture-adapted human embryonic stem cells during long-term culture. Genes. Chromosomes Cancer *47*, 665–679.